© The American Society of Gene Therapy

High-efficiency Transduction of the Mouse Retina by Tyrosine-mutant AAV Serotype Vectors

Hilda Petrs-Silva[1], Astra Dinculescu[1], Qiuhong Li[1], Seok-Hong Min[1], Vince Chiodo[1], Ji-Jing Pang[1], Li Zhong[2], Sergei Zolotukhin[2,3], Arun Srivastava[2,3], Alfred S Lewin[3] and William W Hauswirth[1]

[1]Department of Ophthalmology, University of Florida, Gainesville, Florida, USA; [2]Department of Pediatrics, University of Florida, Gainesville, Florida, USA; [3]Department of Molecular Genetics and Microbiology, University of Florida, Gainesville, Florida, USA

Vectors derived from adeno-associated viruses (AAVs) have become important gene delivery tools for the treatment of many inherited ocular diseases in well-characterized animal models. Previous studies have determined that the viral capsid plays an essential role in the cellular tropism and efficiency of transgene expression. Recently, it was shown that phosphorylation of surface-exposed tyrosine residues from AAV2 capsid targets the viral particles for ubiquitination and proteasome-mediated degradation, and mutations of these tyrosine residues lead to highly efficient vector transduction *in vitro* and *in vivo*. Because the tyrosine residues are highly conserved in other AAV serotypes, in this study we evaluated the intraocular transduction characteristics of vectors containing point mutations in surface-exposed capsid tyrosine residues in AAV serotypes 2, 8, and 9. Several of these novel AAV mutants were found to display a strong and widespread transgene expression in many retinal cells after subretinal or intravitreal delivery compared with their wild-type counterparts. For the first time, we show efficient transduction of the ganglion cell layer by AAV serotype 8 or 9 mutant vectors, thus providing additional tools besides AAV2 for targeting these cells. These enhanced AAV vectors have a great potential for future therapeutic applications for retinal degenerations and ocular neovascular diseases.

Received 30 August 2008; accepted 6 November 2008; published online 16 December 2008. doi:10.1038/mt.2008.269

INTRODUCTION

Recombinant adeno-associated viral (rAAV) vectors are derived from the nonpathogenic virus belonging to the Dependovirus genus of the Parvoviridae family.[1] Wild-type (WT) AAVs contain a linear single-stranded DNA genome of ~4.7 kb enclosed within a capsid with icosahedral symmetry, composed of three proteins VP1, VP2, and VP3.[2] In recombinant vectors, genes encoding four replication and three capsid proteins from the WT AAV genome are replaced by a promoter-therapeutic transgene cassette, flanked by the normal AAV inverted terminal repeats required for packaging and replication. Twelve distinct serotypes (AAV1–AAV12) have been described so far, each containing a different capsid amino acid sequence, with over 100 variants in humans and nonhuman primates.[3–6]

The rAAV vectors have been used in many gene therapy studies in the past decade due primarily to several favorable biological features including their lack of pathogenicity, low immunogenicity, lack of viral coding sequences, broad tropism, and their ability to support strong and persistent transgene expression.[7,8] In general, most studies have used pseudotyped vectors, in which the transgene and the promoter of interest are flanked by the 145-bp AAV2 inverted terminal repeats and packaged into different capsid serotypes.[9] These hybrid vectors have enabled the exploration of cellular tropism in various organs, dictated by the amino acid sequence of the parental capsid proteins of distinct serotypes. In addition, recombinant capsid proteins have been generated by DNA-shuffling techniques followed by panning on cell types of interest.[10] This practice has permitted the *in vitro* evolution of novel viral pseudotypes with increased efficiency for specific tissues.[11]

In parallel with translational studies utilizing AAV vectors, research on basic AAV biology has opened up new insights and has led to the development of new strategies, which aim to improve the transduction efficiency of this gene delivery vehicle. One rate-limiting step, the conversion of single-stranded viral genome to double-stranded AAV DNA, was overcome by the development of self-complementary AAV vectors (scAAV), generated by deletion of the terminal resolution site from one rAAV inverted terminal repeat, preventing the initiation of replication at the mutated end.[12] The scAAV vectors have exhibited increased transduction efficiency in different organs including eye, liver, and brain, though their limited packaging ability prevents their use for larger transgene cassettes.[13–15] A second rate-limiting step, the ubiquitination of viral capsid proteins, which promotes degradation of the vector before it reaches the nucleus, also interferes with rAAV2 transduction.[16,17] This phenomenon has been seen in different systems including lung and endothelial cells, and with different serotypes, such as rAAV2, 5, 7, and 8, so far.[18,19]

Previous studies have shown that a cellular chaperone protein, FK506-binding protein (FKBP52), phosphorylated at tyrosine residues by epidermal growth factor receptor protein tyrosine kinase (EGFR-PTK), inhibits AAV2 second-strand DNA synthesis and transgene expression.[20,21] However, inhibition of EGFR-PTK

Correspondence: *Hilda Petrs-Silva, Department of Ophthalmology, University of Florida, 1600 SW Archer Road, Gainesville, Florida 32610-0284, USA. E-mail: hildasilva@ufl.edu*

© The American Society of Gene Therapy

signaling improved the transduction efficiency of both ssAAV and scAAV vectors, suggesting that EGFR-PTK signaling affects other aspects of AAV transduction and not just the second-strand synthesis. It was then shown that inhibition of tyrosine phosphorylation by a specific EGFR-PTK inhibitor decreased ubiquitination of AAV2 capsids, thereby facilitating nuclear transport of ssAAV or scAAV vectors and consequently improving transduction.[22] Based on these results, the next generation of AAV vectors were recently designed containing single-point mutations of surface-exposed tyrosine residues in the AAV2 VP3 capsids, and highly efficient transduction could be achieved in human cells *in vitro* and in murine hepatocytes *in vivo*.[23]

In the eye, rAAV vectors are established gene delivery tools for the treatment of many inherited retinal degenerations and ocular neovascular diseases in well-characterized animal models, mainly because of their low immunogenicity, the ability to target the majority of nondividing retinal cells affected by disease, and to efficiently express a therapeutic gene for a long period of time following a single treatment.[24] Monogenic diseases characterized by a slow loss of photoreceptor cells allowing a well-preserved retinal structure at the time of vector delivery, such as one type of Leber Congenital Amaurosis (LCA2) caused by mutations in RPE65 or X-linked retinoschisis, due to the absence of functional retinoschisin protein, have shown the best responses to therapy.[25,26] Three recent clinical trials for the LCA2 have reported early promising results in this severe childhood-onset retinal disease.[27–30] However, improvement of the currently available gene therapy vectors is always desirable, especially for those diseases characterized by an early onset and quick retinal deterioration which could benefit from achieving rapid, high levels of transgene expression in the affected cells. Furthermore, AAV does elicit the formation of neutralizing antibodies to capsid proteins, which may limit the effectiveness of subsequent treatments if high doses are employed in the initial treatment.[31]

The purpose of this study was to evaluate the intraocular transduction characteristics of the next generation of AAV vectors containing point mutations in surface-exposed and highly conserved capsid tyrosine residues on scAAV serotypes 2, 8, and 9. Expression of the enhanced green fluorescent protein (EGFP) under the control of a small chicken β-actin (smCBA) promoter was examined either after intravitreal or subretinal delivery of each tyrosine-mutant AAV serotype vector and compared to its WT counterpart. In addition, we also optimized the vector dose following intravitreal injections, as this route of delivery has the potential to raise an immune response against AAV capsid proteins.[32]

RESULTS

Retinal ganglion cell transduction

In an effort to enhance the potential of AAV vectors for ocular gene therapy, we analyzed tyrosine-to-phenylalanine capsid

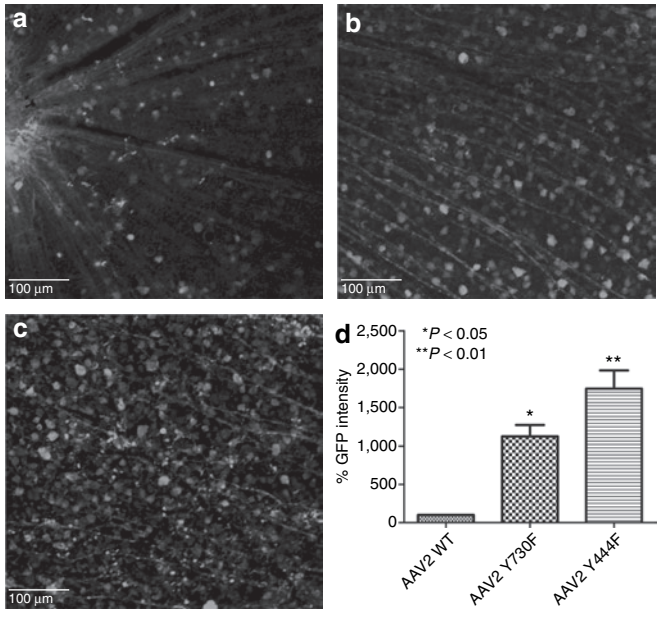

Figure 1 Analysis of enhanced green fluorescent protein (EGFP) expression 2 weeks after intravitreal delivery of equal doses of wild-type (WT) scAAV2-CBA-EGFP or its tyrosine mutants. (**a–c**) Immunohistochemistry for EGFP in flat-mount retinas infected with (**a**) WT AAV2 vector, (**b**) mutant Y730F, or (**c**) mutant Y444F. Calibration bar 100 µm. All pictures were taken with the same exposure time to evaluate EGFP intensity using ImageJ. (**d**) Values indicate percentage of EGFP intensity of the mutants compared with WT. Both type 2 tyrosine mutants showed a statistically significant increase in EGFP intensity with $*P < 0.05$ for Y730F; $**P < 0.01$ for Y444F versus WT AAV2. Statistical analyses were performed with one-way ANOVA plus Dunnett's multiple-range test compared to the control group (WT scAAV2). CBA, chicken β-actin; scAAV, self-complementary adeno-associated virus.

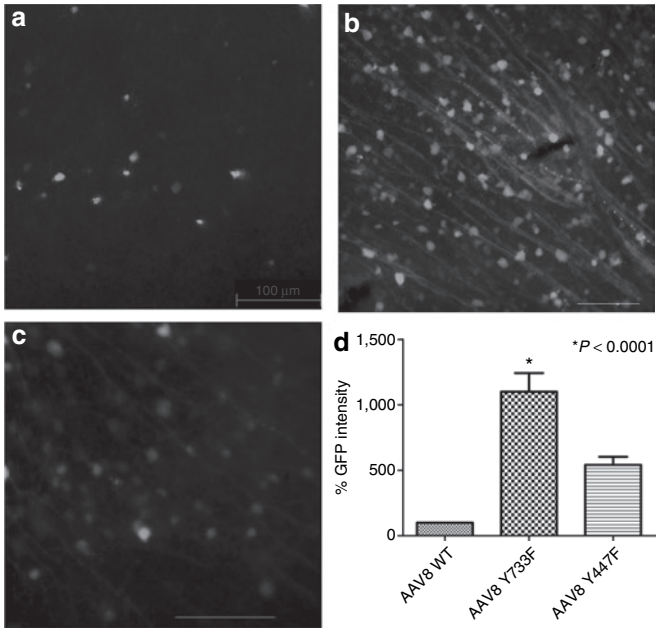

Figure 2 Analysis of enhanced green fluorescent protein (EGFP) expression 2 weeks after intravitreal delivery of equal doses of wild-type (WT) scAAV8-CBA-EGFP or its tyrosine mutants. (**a–c**) Immunohistochemistry for EGFP in flat-mount retinas infected with WT (**a**) AAV8 vector, (**b**) mutant Y733F, or (**c**) mutant Y447F. Calibration bar 100 µm. All pictures were taken with the same exposure time to evaluate EGFP intensity with ImageJ. (**d**) Values indicate percentage of EGFP intensity of the mutants compared with WT. Only tyrosine-mutant Y733F showed a statistically significant elevation in EGFP intensity ($*P < 0.0001$) compared with WT AAV8. Statistical analyses were performed with one-way ANOVA plus Dunnett's multiple-range test compared to the control group (WT scAAV8). CBA, chicken β-actin; scAAV, self-complementary adeno-associated virus.

© The American Society of Gene Therapy

mutants of different serotypes delivered into the retina. Initially, we evaluated the ganglion cell transduction characteristics of two tyrosine-mutant vectors for each serotype 2, 8, and 9. Transgene expression was analyzed by immunofluorescence to best evaluate the cellular pattern of transduction from different scAAV tyrosine mutants, and to be able to visualize cells with low levels enhanced GFP (EGFP).

One microliter of each scAAV tyrosine mutant containing 1×10^9 total vector genome copies was injected intravitreously and EGFP expression was analyzed in retinal flat mounts after 2 weeks. As expected, scAAV with WT capsids (WT-2) showed widespread EGFP fluorescence, with moderate intensity (**Figure 1a,d**). In contrast, both type 2 tyrosine mutants showed quite high-intensity EGFP fluorescence compared to WT-2. GFP signal emanated from the entire retina and was consistent in each treated eye (**Figure 1b,c**). Moreover, clearly many more cells were transduced with mutant vectors. Mutant Y730F showed more than tenfold (11.3 ± 1.5) and Y444F almost 20-fold higher (17.5 ± 2.3) overall EGFP intensity (**Figure 1d**). Although WT-8 and -9 do not transduce the ganglion cell layer as efficiently as WT-2 vectors, tyrosine-to-phenylalanine mutants overcome this problem (**Figures 2** and **3**). Y733F type 8 showed improved transduction, with more cells transduced and EGFP intensity tenfold higher than its WT counterpart (**Figure 2b,d**). The other mutant, Y447F, showed a fivefold improvement. Capsid mutants of type 9 also showed a considerable improvement in cell number and EGFP intensity compared to WT-9 (**Figure 3**), with Y731F showing a 11-fold and Y446F a 16-fold enhancement over WT-9 GFP intensity (**Figure 3d**).

Recombinant AAV2 has been standard for retinal gene transfer because it transduces many different retinal cell types depending of the site of injection; thus far, it is the only serotype for efficient ganglion cell transduction. For this reason, we used standard WT-2 GFP intensity values as a common reference for all serotypes, WT, and mutants, by collecting all images with the same parameters, followed by analysis with ImageJ software from the National Institutes of Health (**Figure 4**). Among all six tyrosine-to-phenylalanine mutants, four showed a statistically significant improvement compared with WT-2 after Dunnett's multiple comparison test. Of these four, type 9 Y446F displayed an almost 8.9-fold increase in GFP intensity, and type 8 Y733F an approximately tenfold increase. The largest improvement was exhibited by both mutants of serotype 2, with Y444F displaying an almost 20-fold higher GFP intensity than WT-2.

Vector titer

In view of the impressive enhancement in vector transduction promoted by type 2 capsid mutants, it became important to analyze whether these tyrosine mutants were capable of efficient *in vivo* expression of the transgene at reduced vector doses. Injections of three different doses, 10^9 (the original dose), as well as 10^7, and 10^5 total vector genomes (vg) were performed. Upon an initial 100-fold dilution of vector genomes delivered from 10^9 to 10^7, the EGFP expression intensity decreased to similar levels for WT-2 and Y730F (**Figure 5b,d** and **i**). However, type 2 Y444F at the concentration of 10^7 vg still showed ninefold higher GFP intensity than WT-2 at 10^9 vg (**Figure 5f,i**). Even at the lowest concentration of 10^5 vg, mutant Y444F led to GFP expression throughout

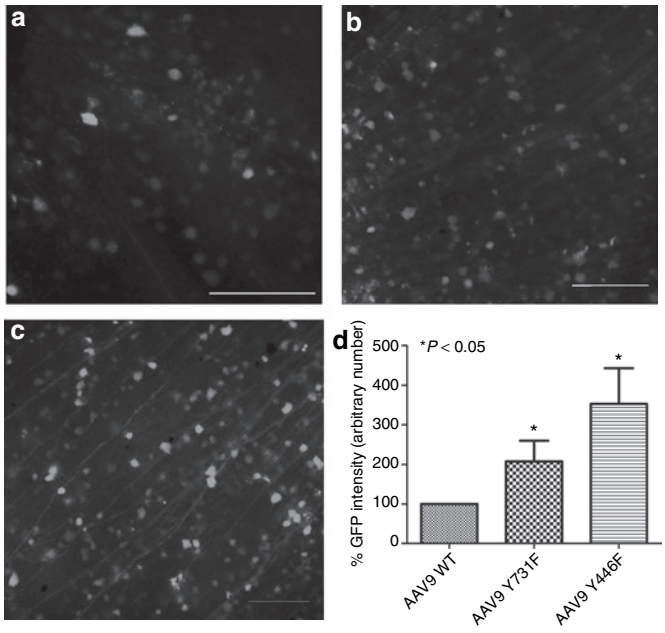

Figure 3 Analysis of enhanced green fluorescent protein (EGFP) expression 2 weeks after equal doses of intravitreal delivery of wild-type self-complementary adeno-associated virus 9 (WT scAAV9) vector or its tyrosine mutants. (**a–c**) Immunohistochemistry for EGFP in flat-mount retinas infected with (**a**) WT AAV9 vector, (**b**) mutant Y731F, or (**c**) mutant Y446F. Calibration bar 100 µm. All pictures were taken with the same exposure time to evaluate EGFP intensity with ImageJ. (**d**) Values indicate percentage of EGFP intensity of the mutants compared with WT. Both tyrosine mutants of type 9 showed statistically significant increase in EGFP intensity with $*P < 0.0001$ for both mutants versus WT AAV9. Statistical analyses were performed with one-way ANOVA plus Dunnett's multiple-range test compared to the control group (WT scAAV9).

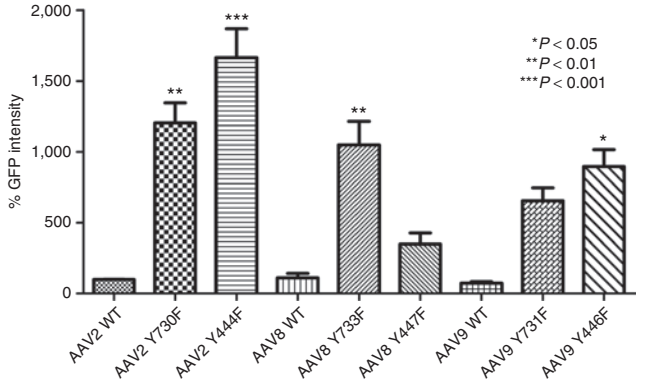

Figure 4 Comparison of enhanced green fluorescent protein (EGFP) intensity of all serotypes and their mutants with wild-type self-complementary adeno-associated virus 2 (WT scAAV2) vector 2 weeks after intravitreal delivery. Retinal flat mounts were immunolabeled with polyclonal EGFP antibody. Pictures were taken with the same exposure time to evaluate the intensity, with ImageJ. Values indicate percentage of EGFP intensity compared with wild-type AAV2 vector. Type 2 Y444F showed the highest GFP expression enhancement ($***P < 0.001$); type 2 mutant Y730F and type 8 Y733F also significantly EGFP expression ($**P < 0.01$); type 9 mutant Y446F also had a higher level of EGFP ($*P < 0.05$). Statistical analyses were performed with one-way ANOVA plus Dunnett's multiple-range test compared to the control group (WT scAAV2).

© The American Society of Gene Therapy

the retina, with an overall fluorescence intensity approximately fourfold higher than WT-2 at the highest concentration of 10^9 vg (**Figure 5g,h** and **i**). Type 8 Y733F and type 9 Y446F were also analyzed in these lower doses; however, at 10^7 vg, both showed weaker EGFP intensity than WT-2 at the same concentration (data not shown).

Retinal penetration following intravitreal injection

In order to analyze the localization of transduction promoted by the two strongest capsid mutants, transverse sections of the retinas treated with type 2 WT, type 2 Y730F, or Y444F mutants were immunostained 2 weeks after intravitreal delivery of 10^9 vg. Both type 2 WT and Y730F showed similar profiles of ganglion cell transduction, and Y444F also displayed widespread EGFP staining throughout the retinal layers (**Figure 6**). No Müller cell transduction pattern was evidently distinguished in our experiments with this vector. Interestingly, the photoreceptor cell layer was consistently transduced by Y444F at the highest titer demonstrating the powerful transduction ability of this mutant (**Supplementary Figure S1**). However, EGFP expression was limited to the ganglion cell layer of the retina when Y444F was delivered at lower titers of 10^7 and 10^5 vg (data not shown).

Gene transfer following subretinal injection

The route of vector administration to the eye largely determines which cells are exposed to the vector and hence limits potential

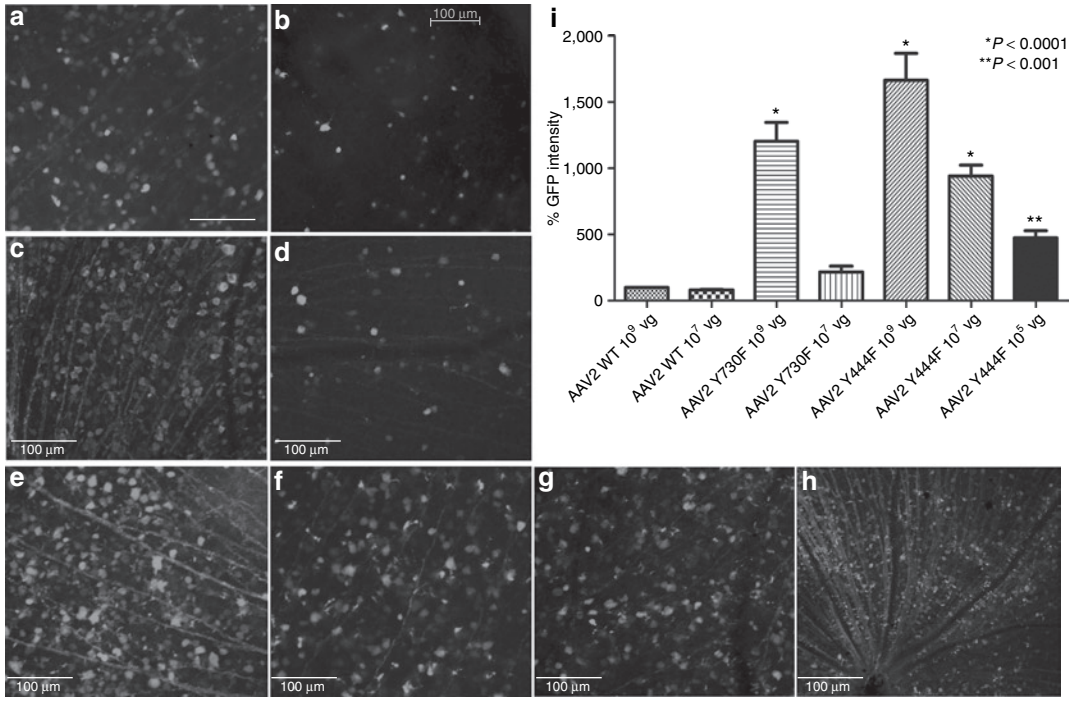

Figure 5 Enhanced green fluorescent protein (EGFP) expression in murine retinas intravitreally injected with serial dilutions of the two strongest mutants compared with wild type (WT). Retina flat-mount immunostained for EGFP 2 weeks after intravitreal delivery of WT-2 at 10^9 vector genomes (vg) (**a**) and 10^7 vg (**b**); mutant Y730F at 10^9 vg (**c**) and 10^7 vg (**d**); and mutant Y444F at 10^9 vg (**e**), 10^7 vg (**f**), and 10^5 vg at higher magnification (**g**) and lower magnification (**h**), providing an assessment of the extent (area) of transduction. Calibration bar 100 µm. EGFP intensity was evaluated with ImageJ and values indicate percentage of EGFP intensity compared with WT adeno-associated virus 2 (AAV2) vector at the standard concentration of 10^9 vg (**i**). Statistical analyses were performed with one-way ANOVA plus Dunnett's multiple-range test compared to the control group (WT scAAV2).

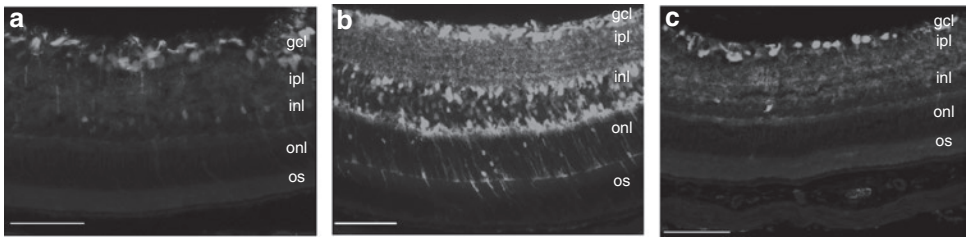

Figure 6 Fluorescence microscopic evaluation of enhanced green fluorescent protein (EGFP) expression in transverse sections of retinal tissue 2 weeks after intravitreal injection. Immunostaining for EGFP in sections of the retina after delivery of (**a**) wild-type self-complementary adeno-associated virus 2 (WT scAAV2), (**b**) serotype 2 tyrosine-mutant Y444F, and (**c**) serotype 2 tyrosine-mutant Y730F. Note intense EGFP staining throughout all retinal layers with Y444F mutant and predominant EGFP staining in the GCL with WT-2 and Y730F. Calibration bar 100 µm. gcl, ganglion cell layer; ipl, inner plexiform layer; inl, inner nuclear layer; onl, outer nuclear; os, outer segment.

© The American Society of Gene Therapy

transduction to only those cells. Gene transfer to retinal pigment epithelial (RPE) or photoreceptors generally requires delivery of vector into the subretinal space. The pattern of cellular transduction, as well as the onset and quantification of the intensity of transgene expression after subretinal delivery have been previously documented for several WT AAV serotypes, including AAV2, 8, and 9.[24,33] Thus, it has been determined that both WT serotypes 8 and 9 display an early onset of transgene expression, and detection of *in vivo* EGFP fluorescence by fundoscopic analysis becomes apparent as early as 5 days after subretinal delivery of self-complementary serotype WT-8, after which it continues to increase, reaching stabilizing levels several weeks later.[34] Consequently, our analysis was focused on establishing if any of the scAAV tyrosine/phenylalanine mutants were more efficient compared to the currently characterized WT scAAV serotypes by using the noninvasive, fundus photography technique. This qualitative approach was used to evaluate the expression of the transgene in live animals, initially at 10 days after vector injection, before EGFP reached saturating levels (**Figure 7**). At this time point, intense and widespread EGFP expression was seen only for the type 8 Y733F mutant (**Figure 7d**), and expression was visible only in patchy areas of the fundus for type 2 Y444F and Y730F, WT-8, WT-9, and type 9 Y446F (**Figure 7a–c,e** and **f**, respectively). WT-2 and type 9 Y731F did not produce detectable fluorescence at this time point. One week after the initial fundoscopic examination, fundus photographs of the above mutant and WT

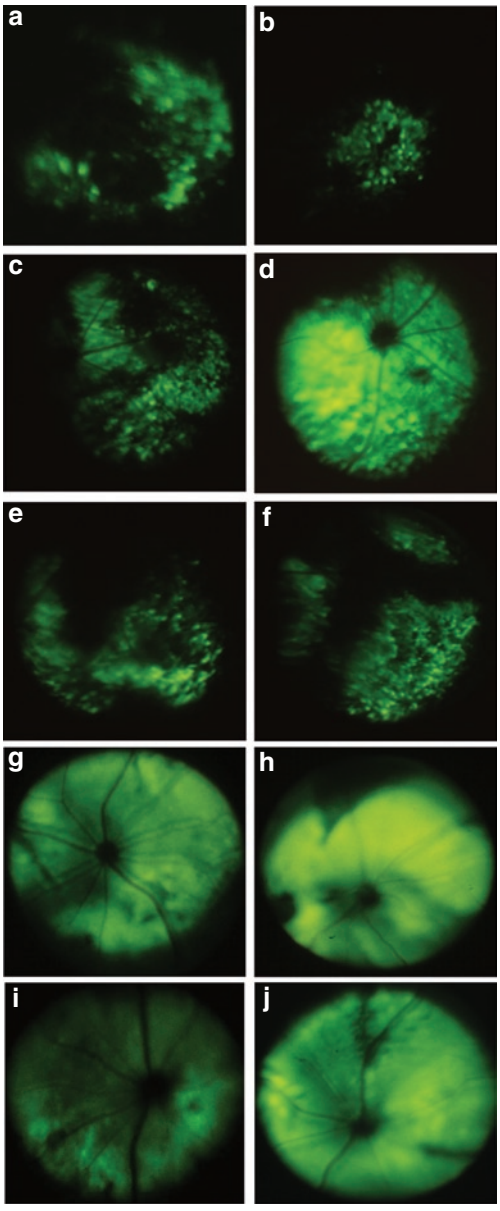

Figure 7 Fundus photos depicting *in vivo* enhanced green fluorescent protein (EGFP) fluorescence in adult mouse retinas after subretinal delivery of scAAV-CBA-EGFP viral vectors. At 10 days postinjection, fluorescence was the strongest and most widespread for serotype 8 Y733F (**d**), and it was only seen in patchy areas of the fundus for serotype 2 Y444F (**a**) and Y730F (**b**), wild-type 8 (WT-8) (**c**), WT-9 (**e**), and serotype 9 Y446F (**f**). Representative fundus photographs at 17 days postinjection are shown for WT-8 (**g**), serotype 8 Y733F (**h**), serotype 2 Y444F (**i**), and serotype 9 Y446F (**j**). CBA, chicken β-actin; scAAV, self-complementary adeno-associated virus.

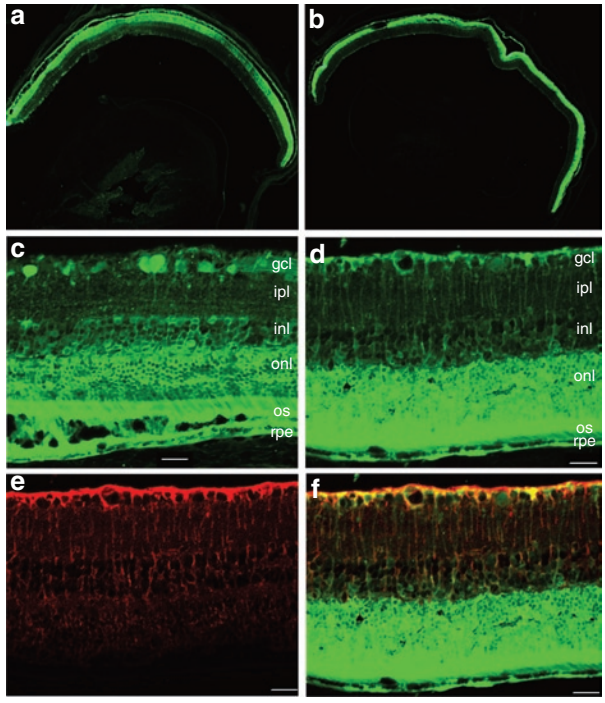

Figure 8 Analysis of enhanced green fluorescent protein (EGFP) expression in frozen retinal sections by immunohistochemistry at 1 month following subretinal injections with highly efficient Tyr/Phe mutant adeno-associated virus vectors. Representative sections depicting widespread and intense EGFP fluorescence throughout the retina after transduction with (**a**) serotype 2 Y444F or (**b**) serotype 8 Y733F. The images are oriented with the vitreous toward the bottom and the photoreceptor layer toward the top. Calibration bar 500 µm. (**c**) EGFP fluorescence in photoreceptors, retinal pigment epithelial (RPE), and ganglion cells from mouse eyes injected subretinally with serotype 2 Y444F; (**d**) EGFP fluorescence in photoreceptors, RPE, and Müller cells after serotype 8 Y733F delivery. (**e**) Detection of Müller cells processes (red) by immunostaining with a glutamine synthetase (GS) antibody. (**f**) Merged image showing colocalization of EGFP fluorescence (green) and GS staining (red) in retinal sections from eyes treated with serotype 8 Y733F. Calibration bar 100 µm. gcl, ganglion cell layer; ipl, inner plexiform layer; inl, inner nuclear layer; onl, outer nuclear; os, outer segment.

© The American Society of Gene Therapy

scAAVs displayed more uniform and widespread fluorescence, with the exception of WT-2, in which no fluorescence could be detected. Representative fundus photographs taken at 17 days postinjection are shown for WT-8, serotype 8 Y733F, serotype 2 Y444F, and serotype 9 Y446F (**Figure 7g–j**, respectively).

Based on these findings, type 2 Y444F and type 8 Y733F, found to be the two most efficient compared to their WT counterparts, were further characterized by immunohistochemistry. Analysis of transgene expression by fluorescent microscopy of frozen retinal sections revealed that subretinal injections of either vector resulted in widespread EGFP transduction throughout the RPE and photoreceptor cells of the mouse retina, as well as many inner retinal cells (**Figure 8**). Type 8 Y733F also transduced Müller cells as seen from colocalization experiments with a specific Müller cell antibody (**Figure 8d–f**). In addition, type 2 Y444F strongly transduced some ganglion cells after subretinal delivery (**Figure 8c**). For both mutant vectors, this transduction pattern was consistent throughout the retina, and not just in a defined area around the injection site where local injury due to the surgical retinotomy had caused inner retinal transduction (**Figure 8a,b**). The immunohistochemistry for Müller cells was also performed for serotype 2 Y444F and no colocalization with EGFP was detected (**Supplementary Figure S2**). It should be noted that these capsid tyrosine mutations do not seem to change the cellular tropism of the vectors relative to their WT counterparts, but rather they enhance their transduction potential by allowing their escape from proteasome-mediated degradation, leading to increased reporter gene expression in target cells that otherwise would remain undetected.

DISCUSSION

The efficiency of rAAV transduction is dependent on multiple steps involving virus–host cell interactions, which include binding to cellular receptors, overcoming intracellular barriers that limit nuclear accumulation of the virus and the conversion of single-stranded viral genomes to double-stranded forms.[35] As previously noted, the capsid is an essential element that influences both the extracellular events related to the recognition of specific receptors and intracellular processes affecting the AAV trafficking and uncoating. Thus, the capsid plays an essential role in the cellular tropism, transduction kinetics, and intensity of efficiency of transgene expression.[36,37] Modulating these properties can improve both the effectiveness and safety of gene therapy, and the use of the appropriate combinations of cellular promoters and AAV vector serotypes have enabled the targeted expression of the transgene of interest in specific cells.

In the retina, AAV serotypes 1–9 have been characterized in previous studies, and a few were found to display robust transgene expression in the retinal ganglion cell layer, the RPE, and rod and cone photoreceptors.[24] For example, the tropism of AAV serotypes 1 and 4 was found to be directed mainly toward the RPE cells,[38,39] and AAV2, 5, 7, 8, and 9 were found to target both RPE and photoreceptors following subretinal injections.[37,40,41] Of these, serotypes 5, 7, 8, and 9 exhibited faster transgene expression and more efficient transduction than type 2 after subretinal delivery, with AAV8 displaying a widespread and robust cellular transduction according to recent studies.[34,42] However, only AAV2 serotype has been found to efficiently transduce ganglion cells after intravitreal injections. Some transduction of internal retinal cell layers has also been seen after intravitreal or subretinal delivery of scAAV2 in mouse eyes.[14]

In this article, we describe the transduction efficiency of the next generation of scAAV vectors, surface-exposed capsid tyrosine mutants for serotypes 2, 8, and 9, so far the only serotypes generated. We have chosen to produce these self-complementary vectors based on the enhanced *in vivo* performance of serotypes 8 and 9, as determined by previous studies. We document that both mutants of AAV type 2, Y444F and Y730F, and mutant Y733F in AAV type 8, and mutant Y446F in AAV type 9 enhance the efficiency of transduction in the retinal ganglion cell layer after intravitreal injection. This is the first time that alternatives to WT AAV2 have become available for promoting strong and widespread transgene expression in retinal ganglion cells. In addition, Y444F at the highest titer was able to transduce photoreceptors consistently throughout the retina after intravitreal injection.

Tyrosine phosphorylation serves as a signal for ubiquitination of intact AAV particles, leading to subsequent targeting for the proteasome-mediated vector degradation before reaching the nucleus. In this context, mutation of capsid tyrosine residues from either ss or scAAV particles is predicted to allow the vectors to escape the proteasome degradation pathway and thus promote more vector genome delivery to the nucleus and more aggressive transgene expression. A recent study has indeed shown that *in vitro* phosphorylation of viral capsids at tyrosine residues significantly decreases the transduction efficiency of both ssAAV2 and scAAV2, and the intracellular trafficking from the cytoplasm to the nucleus.[43] Our results demonstrating potentiation of vector transduction on mutation of capsid tyrosines suggest that the ubiquitin pathway is also likely to be involved in AAV transduction of retinal cells, and that, by minimizing intracellular capsid phosphorylation, these mutants are able to escape the proteasome degradation pathway, thus promoting more efficient transgene expression.

In addition to expanding the availability of rAAVs for targeting the ganglion cell layer, the existence of different serotypes with unique immunological properties may offer an alternate pathway for those cases in which the efficiency of gene therapy could be hindered by existing neutralizing anti-AAV2 antibodies, which are prevalent in the human population.[31,44] Among the factors that were found to influence the immunological responses against rAAV vectors in gene therapy studies in general were preexisting immunity to a specific WT AAV serotype, the route of rAAV administration, and the vector dose.[33] Recent studies performed by Li *et al.*[32] have demonstrated that a humoral immune response against serotype 2 AAV capsid proteins is a function of the route of AAV administration. That study provided evidence for a systemic antibody-mediated response against AAV2 capsid proteins following the intravitreal but not subretinal delivery of vector.

In this study, we also determined the dependence of ganglion cell transduction on the dose of intravitreal vector delivered. For the most potent mutant, type 2 Y444F, even further reduction to 10^5 vg delivered from the initial 10^9, has resulted in widespread and intense expression of the transgene. At this 10,000-fold reduction in the number of vector particles, Y444F still performed better

© The American Society of Gene Therapy

than WT AAV2 at the highest concentration of 10^9 vg. Using this efficient mutant should enable a lower viral dose to attain the same therapeutic transgene levels as WT AAV2, thus minimizing immunological responses against the viral capsid. A recent study using AAV1 has indeed shown that the level of neutralizing antibody is proportional to the virus dose and that preexisting serum antibody reduces the efficiency of transgene expression following readministration of the vector.[45] The range of application for rAAV vectors mediating retinal gene therapy after intravitreal delivery is, therefore, likely to be expanded. This could be achieved either by using lower titers of the highly efficient AAV2 Y444F capsid mutant to minimize or avoid systemic immune response or, if necessary, by using a different serotype, such as mutant AAV8 or 9 in cases where repeated treatments are desired.

The qualitative transduction pattern after subretinal delivery of the scAAV2, 8, and 9 mutant serotypes is similar, with both RPE and photoreceptors being efficiently transduced. Subretinal delivery typically involves a small volume of AAV vector (usually 1 µl for mouse) in the virtual space between the RPE layer and the photoreceptor outer segments, thus creating a temporary retinal detachment. The area of the detachment essentially defines the area of transduced cells; however, both scAAV2 Y444F and scAAV8 Y733F appeared to support higher levels of transgene expression, as determined by early fundoscopic examination of GFP fluorescence compared to WT AAV2 or WT AAV8. This is consistent with the concept that these mutants evade proteasome degradation allowing more transgene copies to enter the nucleus and express transgene protein. Thus, those diseases that require fast and high levels of transgene expression in photoreceptors or RPE cells would benefit from using AAV-Tyr/Phe mutants because subretinal delivery of rAAV does appear not to trigger neutralizing antibodies against AAV capsid.[32] Moreover, a variety of inner retinal cells were also transduced by some of these mutant vectors. This property might be beneficial in those cases of retinal degeneration in which the majority of photoreceptors have already been lost, and efficient transduction of the inner retinal cells with light-absorbing chromophores may be required to generate a light response.[46]

The scAAV2 Y444F mutant also targeted the majority of ganglion cells after subretinal injection, and Müller cells were transduced well by scAAV8 Y733F mutant (**Figure 8** and **Supplementary Figure S2**). This pattern was consistent in all analyzed sections from all treated eyes, indicating that widespread diffusion occurs in the retina after subretinal delivery of these vectors, and suggesting that their high efficiency of transduction allows the visualization of transgene expression in target cells. Another recent study showed that Müller cells can also be transduced by scAAV9, and to a lesser extent by scAAV8 after subretinal delivery, though panretinal distribution of GFP expression has not been demonstrated in these cases.[40] Müller cells span the entire retinal tissue from the inner to the outer limiting membranes, and among their many functions; they can modulate the survival of retinal neurons by releasing a variety of neurotrophic factors. The possibility of efficiently targeting Müller cells opens up new therapeutic possibilities for the treatment of ocular diseases that affect any layer of the retina. A previous study showed that subretinal, but not intravitreal delivery of lentiviral vectors containing the glial fibrillary acidic protein (GFAP) promoter led to high-level transgene expression in Müller cells.[47] Similar to that study, we noticed that Müller cell transduction by serotype 8 occurs only through the subretinal delivery route, and not the intravitreal one.

These optimized capsid-mutant AAV vectors have the potential to become important tools for retinal gene-transfer studies for mechanistic questions as well as for therapeutic applications in a variety of ocular diseases involving the retina. Although this study has employed the robust and non–cell-specific CBA promoter to visualize the GFP expression throughout the retina, the use of cell-specific promoters and regulatory elements to limit transgene expression to subsets of retinal cells may be necessary for safe gene therapy applications that reach the correct target and to minimize potential detrimental side effects caused by transgene misexpression and overexpression. Studies are currently underway to determine the potential of these highly efficient Tyr/Phe mutant vectors for the treatment of ocular diseases in established animal models, and to establish if the immune response can be effectively circumvented by the use of alternative or low-titer AAV vectors after intravitreal delivery.

MATERIALS AND METHODS

Generation of rAAV vectors. Site-directed mutagenesis of surface-exposed tyrosine residues on the AAV2 capsids has been described recently.[23] Similar strategies were used to generate AAV serotypes 8 and 9 vectors containing tyrosine-to-phenylalanine mutations.

Vector preparations were produced by the plasmid cotransfection method.[48] The crude iodixanol fraction, as described, was further purified and concentrated by column chromatography on a 5-ml HiTrap Q Sepharose column using a Pharmacia AKTA FPLC system (Amersham Biosciences, Piscataway, NJ). The vector was eluted from the column using 215 mM NaCl, pH 8.0, and the rAAV peak collected. Vector-containing fractions were then concentrated and buffer exchanged in Alcon BSS with 0.014% Tween 20, using a Biomax 100 K concentrator (Millipore, Billerica, MA). Vector was then titered for DNase-resistant vector genomes by real-time PCR relative to a standard. Finally, the purity of the vector was validated by silver-stained sodium dodecyl sulfate–polyacrylamide gel electrophoresis, assayed for sterility and lack of endotoxin, and then aliquoted and stored at −80 °C.

Intraocular administration routes. Adult C57BL/6 mice were used for all studies. All procedures in animals were handled according to the statement for the use of animals in Ophthalmic and Vision Research of the Association of Research in Vision and Ophthalmology and the guidelines of the Institutional Animal Care and Use Committee at the University of Florida. Before vector administration, mice were anesthetized with ketamine (72 mg/kg)/xylazine (4 mg/kg) by intraperitoneal injection. A Hamilton syringe fitted with a 33-gauge beveled needle was used for intravitreal injection. The needle was passed through the sclera, at the equator, next to the *limbus*, into the vitreous cavity. Injection occurred with direct observation of the needle in the center of the vitreous cavity. The total volume delivered was 1 µl, containing different concentrations of the AAV tested. Subretinal injections were performed as described previously.[49] One hour before the anesthesia, the eyes were dilated with eye drops of 1% atropine, followed by topical administration of 2.5% phenylephrine. An aperture within the pupil was made through the cornea with a 30 1/2-gauge disposable needle and a 33-gauge unbeveled blunt needle in a Hamilton syringe was introduced through the corneal opening into the subretinal space and 1 µl of AAV (10^8 vg total) was delivered. More than five mice were injected with each vector in this experiment.

© The American Society of Gene Therapy

Fundus photography. Fundus photographs of mice were taken with a Kowa Genesis digital camera connected to a dissecting microscope after anesthetizing the animals and dilating their pupils.

Flat mounts and cryosections. Two weeks after vector injection, mice were humanely euthanized, the eyes were removed and fixed with 4% paraformaldehyde in phosphate-buffered saline for 1 hour and the cornea and lens were removed. To make flat mounts, the entire retina was carefully dissected from the eyecup and radial cuts were made from the edges to the equator of the retina. For cryosections, the eyecups were washed in phosphate-buffered saline followed by 30% sucrose in the same buffer overnight. Eyes were then embedded in optimal cutting temperature embedding compound (Miles Diagnostics, Elkhart, IN) and oriented for 10-μm thick transverse retinal sections.

Immunolabeling and histological analysis. Flat-mount retinas were incubated with 0.5% Triton X-100 for 1 hour followed by incubation with a blocking solution of 0.5% Triton X-100 and 1% albumin for 1 hour. The retinas were incubated with a commercial mouse monoclonal antibody raised against the GFP (Invitrogen, Molecular Probes, Carlsbad, CA) at 1:400 in blocking solution, overnight at room temperature in a slow orbital shaker. Tissue sections were incubated with 0.5% Triton X-100 for 15 minutes, then washed three times with phosphate-buffered saline for 5 minutes each, followed by incubation with a blocking solution of 1% albumin for 30 minutes. The sections were incubated with the same mouse monoclonal antibody against GFP at 1:400, overnight at 37 °C. Müller cells were detected with an antibody against glutamine synthetase (Abcam, Cambridge, MA). Fluorescent staining was done with an anti-mouse IgG secondary antibody Alexa-fluor 488 (Molecular Probes) by incubating sections for 2 hours at room temperature. The results were examined by fluorescence microscopy using an Axiophot microscope (Zeiss, Thornwood, NY).

GFP intensity analysis. Flat mounts were examined by fluorescence microscopy. Digital pictures were taken with a camera connected to the Axiophot microscope. The ImageJ (National Institutes of Health) software was used to measure the fluorescence intensity in pixels per area.

Statistical analysis. Differences between groups were evaluated with GraphPad Prism software (GraphPad, La Jolla, CA) using one-way ANOVA followed by Dunnett's post-test for group comparison. At least 15 mice were injected per each WT serotype and mutant.

SUPPLEMENTARY MATERIAL

Figure S1. Representative retinal section depicting EGFP fluorescence throughout the entire retina 2 weeks after intravitreal delivery of serotype 2 tyrosine-mutant Y444F.

Figure S2. EGFP expression in retinal sections at 1 month following subretinal injections with serotype 8 Y733F (a,b), or serotype 2 Y444F (c,d).

ACKNOWLEDGMENTS

We acknowledge the National Institutes of Health grants EY11123, EY13729, EY07132, EY08571, EY11087, EY0667, EY018335, NS36302, and grants from Foundation Fighting Blindness, Macular Vision Research Foundation, Research to Prevent Blindness, Inc. and CNPq for partial support to this work. We thank Min Ding, Thomas Andresen, Tom Doyle, and Doug Smith for their technical assistance.

REFERENCES

1. Goncalves, MA (2005). Adeno-associated virus: from defective virus to effective vector. *Virol J* **2**: 43.
2. Xie, Q, Bu, W, Bhatia, S, Hare, J, Somasundaram, T, Azzi, A *et al.* (2002). The atomic structure of adeno-associated virus (AAV-2), a vector for human gene therapy. *Proc Natl Acad Sci USA* **99**: 10405–10410.
3. Gao, G, Vandenberghe, LH, Alvira, MR, Lu, Y, Calcedo, R, Zhou, X *et al.* (2004). Clades of adeno-associated viruses are widely disseminated in human tissues. *J Virol* **78**: 6381–6388.
4. Schmidt, M, Voutetakis, A, Afione, S, Zheng, C, Mandikian, D and Chiorini, JA (2008). Adeno-associated virus type 12 (AAV12): a novel AAV serotype with sialic acid- and heparan sulfate proteoglycan-independent transduction activity. *J Virol* **82**: 1399–1406.
5. Wu, Z, Asokan, A and Samulski, RJ (2006). Adeno-associated virus serotypes: vector toolkit for human gene therapy. *Mol Ther* **14**: 316–327.
6. Mori, S, Wang, L, Takeuchi, T and Kanda, T (2004). Two novel adeno-associated viruses from cynomolgus monkey: pseudotyping characterization of capsid protein. *Virology* **330**: 375–383.
7. Mueller, C and Flotte, TR (2008). Clinical gene therapy using recombinant adeno-associated virus vectors. *Gene Ther* **15**: 858–863.
8. Buning, H, Perabo, L, Coutelle, O, Quadt-Humme, S and Hallek, M (2008). Recent developments in adeno-associated virus vector technology. *J Gene Med* **10**: 717–733.
9. Rabinowitz, JE, Rolling, F, Li, C, Conrath, H, Xiao, W, Xiao, X *et al.* (2002). Cross-packaging of a single adeno-associated virus (AAV) type 2 vector genome into multiple AAV serotypes enables transduction with broad specificity. *J Virol* **76**: 791–801.
10. Kwon, I and Schaffer, DV (2008). Designer gene delivery vectors: molecular engineering and evolution of adeno-associated viral vectors for enhanced gene transfer. *Pharm Res* **25**: 489–499.
11. Muzyczka, N and Warrington, KH Jr (2005). Custom adeno-associated virus capsids: the next generation of recombinant vectors with novel tropism. *Hum Gene Ther* **16**: 408–416.
12. McCarty, DM, Fu, H, Monahan, PE, Toulson, CE, Naik, P and Samulski, RJ (2003). Adeno-associated virus terminal repeat (TR) mutant generates self-complementary vectors to overcome the rate-limiting step to transduction *in vivo*. *Gene Ther* **10**: 2112–2118.
13. McCarty, DM (2008). Self-complementary AAV vectors advances and applications. *Mol Ther* **16**: 1648–1656.
14. Yokoi, K, Kachi, S, Zhang, HS, Gregory, PD, Spratt, SK, Samulski, RJ *et al.* (2007). Ocular gene transfer with self-complementary AAV vectors. *Invest Ophthalmol Vis Sci* **48**: 3324–3328.
15. Wang, Z, Ma, HI, Li, J, Sun, L, Zhang, J and Xiao, X (2003). Rapid and highly efficient transduction by double-stranded adeno-associated virus vectors *in vitro* and *in vivo*. *Gene Ther* **10**: 2105–2111.
16. Duan, D, Yue, Y, Yan, Z, Yang, J and Engelhardt, JF (2000). Endosomal processing limits gene transfer to polarized airway epithelia by adeno-associated virus. *J Clin Invest* **105**: 1573–1587.
17. Douar, AM, Poulard, K, Stockholm, D and Danos, O (2001). Intracellular trafficking of adeno-associated virus vectors: routing to the late endosomal compartment and proteasome degradation. *J Virol* **75**: 1824–1833.
18. Denby, L, Nicklin, SA and Baker, AH (2005). Adeno-associated virus (AAV)-7 and -8 poorly transduce vascular endothelial cells and are sensitive to proteasomal degradation. *Gene Ther* **12**: 1534–1538.
19. Yan, Z, Zak, R, Luxton, GW, Ritchie, TC, Bantel-Schaal, U and Engelhardt, JF (2002). Ubiquitination of both adeno-associated virus type 2 and 5 capsid proteins affects the transduction efficiency of recombinant vectors. *J Virol* **76**: 2043–2053.
20. Qing, K, Hansen, J, Weigel-Kelley, KA, Tan, M, Zhou, S and Srivastava, A (2001). Adeno-associated virus type 2-mediated gene transfer: role of cellular FKBP52 protein in transgene expression. *J Virol* **75**: 8968–8976.
21. Qing, K, Li, W, Zhong, L, Tan, M, Hansen, J, Weigel-Kelley, KA *et al.* (2003). Adeno-associated virus type 2-mediated gene transfer: role of cellular T-cell protein tyrosine phosphatase in transgene expression in established cell lines *in vitro* and transgenic mice *in vivo*. *J Virol* **77**: 2741–2746.
22. Zhong, L, Zhao, W, Wu, J, Li, B, Zolotukhin, S, Govindasamy, L *et al.* (2007). A dual role of EGFR protein tyrosine kinase signaling in ubiquitination of AAV2 capsids and viral second-strand DNA synthesis. *Mol Ther* **15**: 1323–1330.
23. Zhong, L, Li, B, Mah, CS, Govindasamy, L, Abandje-McKenna, M, Cooper, M *et al.* (2008). Next generation of adeno-associated virus 2 vectors: point mutations in tyrosines lead to high-efficiency transduction at lower doses. *Proc Natl Acad Sci USA* **105**: 7827–7832.
24. Surace, EM and Auricchio, A (2008). Versatility of AAV vectors for retinal gene transfer. *Vision Res* **48**: 353–359.
25. Acland, GM, Aguirre, GD, Ray, J, Zhang, Q, Aleman, TS, Cideciyan, AV *et al.* (2001). Gene therapy restores vision in a canine model of childhood blindness. *Nat Genet* **28**: 92–95.
26. Min, SH, Molday, LL, Seeliger, MW, Dinculescu, A, Timmers, AM, Janssen, A *et al.* (2005). Prolonged recovery of retinal structure/function after gene therapy in an Rs1h-deficient mouse model of x-linked juvenile retinoschisis. *Mol Ther* **12**: 644–651.
27. Bainbridge, JW, Smith, AJ, Barker, SS, Robbie, S, Henderson, R, Balaggan, K *et al.* (2008). Effect of gene therapy on visual function in Leber's congenital amaurosis. *N Engl J Med* **358**: 2231–2239.
28. Maguire, AM, Simonelli, F, Pierce, EA, Pugh, EN Jr, Mingozzi, F, Bennicelli, J *et al.* (2008). Safety and efficacy of gene transfer for Leber's congenital amaurosis. *N Engl J Med* **358**: 2240–2248.
29. Cideciyan, AV, Aleman, TS, Boye, SL, Schwartz, SB, Kaushal, S, Roman, AJ *et al.* (2008). Human gene therapy for, RPE65 isomerase deficiency activates the retinoid cycle of vision but with slow rod kinetics. *Proc Natl Acad Sci USA* **105**: 15112–15117.
30. Hauswirth, W, Aleman, TS, Kaushal, S, Cideciyan, AV, Schwartz, SB, Wang, L *et al.* (2008). Phase I trial of leber congenital amaurosis due to RPE65 mutations by ocular subretinal injection of adeno-associated virus gene vector: short-term results. *Hum Gene Ther* (epub ahead of print).
31. Zaiss, AK and Muruve, DA (2008). Immunity to adeno-associated virus vectors in animals and humans: a continued challenge. *Gene Ther* **15**: 808–816.
32. Li, Q, Miller, R, Han, PY, Pang, J, Dinculescu, A, Chiodo, V *et al.* (2008). Intraocular route of AAV2 vector administration defines humoral immune response and therapeutic potential. *Mol Vis* **14**: 1760–1769.
33. Vandenberghe, LH and Wilson, JM (2007). AAV as an immunogen. *Curr Gene Ther* **7**: 325–333.
34. Natkunarajah, M, Trittibach, P, McIntosh, J, Duran, Y, Barker, SE, Smith, AJ *et al.* (2008). Assessment of ocular transduction using single-stranded and self-complementary recombinant adeno-associated virus serotype 2/8. *Gene Ther* **15**: 463–467.

© The American Society of Gene Therapy

35. Schultz, BR and Chamberlain, JS (2008). Recombinant adeno-associated virus transduction and integration. *Mol Ther* **16**: 1189–1199.
36. Surace, EM and Auricchio, A (2003). Adeno-associated viral vectors for retinal gene transfer. *Prog Retin Eye Res* **22**: 705–719.
37. Yang, GS, Schmidt, M, Yan, Z, Lindbloom, JD, Harding, TC, Donahue, BA *et al.* (2002). Virus-mediated transduction of murine retina with adeno-associated virus: effects of viral capsid and genome size. *J Virol* **76**: 7651–7660.
38. Weber, M, Rabinowitz, J, Provost, N, Conrath, H, Folliot, S, Briot, D *et al.* (2003). Recombinant adeno-associated virus serotype 4 mediates unique and exclusive long-term transduction of retinal pigmented epithelium in rat, dog, and nonhuman primate after subretinal delivery. *Mol Ther* **7**: 774–781.
39. Auricchio, A, Kobinger, G, Anand, V, Hildinger, M, O'Connor, E, Maguire, AM *et al.* (2001). Exchange of surface proteins impacts on viral vector cellular specificity and transduction characteristics: the retina as a model. *Hum Mol Genet* **10**: 3075–3081.
40. Allocca, M, Mussolino, C, Garcia-Hoyos, M, Sanges, D, Iodice, C, Petrillo, M *et al.* (2007). Novel adeno-associated virus serotypes efficiently transduce murine photoreceptors. *J Virol* **81**: 11372–11380.
41. Lebherz, C, Maguire, A, Tang, W, Bennett, J and Wilson, JM (2008). Novel AAV serotypes for improved ocular gene transfer. *J Gene Med* **10**: 375–382.
42. Stieger, K, Colle, MA, Dubreil, L, Mendes-Madeira, A, Weber, M, Le, MG *et al.* (2008). Subretinal delivery of recombinant AAV serotype 8 vector in dogs results in gene transfer to neurons in the brain. *Mol Ther* **16**: 916–923.
43. Zhong, L, Li, B, Jayandharan, G, Mah, CS, Govindasamy, L, gbandje-McKenna, M *et al.* (2008). Tyrosine-phosphorylation of AAV2 vectors and its consequences on viral intracellular trafficking and transgene expression. *Virology* **381**: 194–202.
44. Peden, CS, Burger, C, Muzyczka, N and Mandel, RJ (2004). Circulating anti-wild-type adeno-associated virus type 2 (AAV2) antibodies inhibit recombinant AAV2 (rAAV2)-mediated, but not rAAV5-mediated, gene transfer in the brain. *J Virol* **78**: 6344–6359.
45. Petry, H, Brooks, A, Orme, A, Wang, P, Liu, P, Xie, J *et al.* (2008). Effect of viral dose on neutralizing antibody response and transgene expression after AAV1 vector re-administration in mice. *Gene Ther* **15**: 54–60.
46. Tomita, H, Sugano, E, Yawo, H, Ishizuka, T, Isago, H, Narikawa, S *et al.* (2007). Restoration of visual response in aged dystrophic RCS rats using AAV-mediated channelopsin-2 gene transfer. *Invest Ophthalmol Vis Sci* **48**: 3821–3826.
47. Greenberg, KP, Geller, SF, Schaffer, DV and Flannery, JG (2007). Targeted transgene expression in muller glia of normal and diseased retinas using lentiviral vectors. *Invest Ophthalmol Vis Sci* **48**: 1844–1852.
48. Zolotukhin, S, Byrne, BJ, Mason, E, Zolotukhin, I, Potter, M, Chesnut, K *et al.* (1999). Recombinant adeno-associated virus purification using novel methods improves infectious titer and yield. *Gene Ther* **6**: 973–985.
49. Pang, JJ, Chang, B, Kumar, A, Nusinowitz, S, Noorwez, SM, Li, J *et al.* (2006). Gene therapy restores vision-dependent behavior as well as retinal structure and function in a mouse model of RPE65 Leber congenital amaurosis. *Mol Ther* **13**: 565–572.